Models with a Cause: Causal Discovery with Language Models on Temporally Ordered Text Data

Anonymous authors
Paper under double-blind review

Abstract

While language models (LMs) have been proposed for causal discovery tasks, it remains unclear whether they possess the inductive biases necessary to identify causal structures in token generation processes. We investigate whether LMs can learn the causal structure governing how tokens depend on their predecessors by testing if they possess the temporal and statistical properties required for causal discovery. We prove that existing algorithms can recover a unique causal model when token sequences satisfy standard causal assumptions and have temporal ordering. LMs' sequential processing and positional encodings enable them to leverage this temporal information. Using controlled experiments on synthetic data generated by mixtures of Markov chains, we test whether LMs learn conditional independencies and Markov exchangeability properties necessary for causal discovery. We find that transformers successfully learn these properties, achieving this not by approximating exact probability distributions but by learning qualitative probability rankings. These synthetic experiments provide initial evidence that LMs possess inductive biases suitable for discovering token-level causal structures.

1 Introduction

Recent work has explored using language models (LMs) for causal discovery in code (Li et al., 2024b; Gupta et al., 2023) and natural language (Zhu et al., 2024; Ban et al., 2023). However, a fundamental question remains: do LMs possess the inductive biases necessary to learn causal structures from text data? This question matters because conventional causal discovery algorithms (PC, IC) cannot scale to high-dimensional text data. Moreover, impossibility results (Bareinboim et al., 2022) show that probabilistic models cannot perform causal discovery without appropriate inductive biases. This paper identifies conditions where causal discovery is theoretically possible and tests whether LMs exhibit the required biases. Crucially, we study the causal structure of token generation processes—how words depend on previous words—not the extraction of semantic causal claims from text content (e.g., 'smoking causes cancer'). Understanding token-level causal structure provides a foundation for higher-level causal reasoning tasks.

Consider the the sequence of words ["the", "cat", "sat"]. We ask whether the model learns that the word "sat" depends only on the word "cat" given the causal structure, i.e. altering "cat" changes the distribution from which "sat" is drawn. We are not extracting the semantic claim that cats cause sitting. Token-level causation is analogous to how Markov chains describe state transitions rather than semantic relationships between states.

Our approach leverages a key property of text: human language production is often temporally ordered, with words following their predecessors in time. While exceptions exist (e.g., heavily edited documents), temporal ordering is prevalent in typical training corpora. For example, the text of a recorded conversation will have words follow one-another temporally. LMs use positional encodings that enable them to detect token ordering, including temporal sequences. This contrasts with traditional causal discovery methods that operate on unordered tabular data.

We prove that temporal information enables unique causal model recovery under standard assumptions (Markov, minimal, faithful, no hidden confounders). Specifically, temporal ordering resolves the equivalence

class produced by conditional independence-based algorithms like PC down to a unique model. Thus, causal discovery from text requires two inductive biases: learning conditional independencies and detecting temporal order. While LMs can encode temporal information through positional encodings, the key empirical question is whether they learn the conditional independence patterns or symmetry properties necessary for causal discovery. Testing on natural text is challenging because the true causal structure is unknown. We therefore use synthetic datasets with known causal structures as a necessary baseline: if LMs cannot learn these patterns in controlled settings, they cannot learn them in real text. We find that Transformer variants can identify the required probabilistic properties under specific conditions, suggesting they possess the inductive biases for causal discovery. Surprisingly, models achieve this without accurately approximating the data distribution—they learn *qualitative probability rankings* rather than exact probabilities.

Our contributions are: (1) We prove temporal information enables unique recovery of certain causal structures, (2) we test four architectures on synthetic Markov chain mixtures for required inductive biases, (3) we demonstrate that Encoder-Decoder, Decoder-only, and Switch transformers learn Markov exchangeability, and (4) we show models learn qualitative probability rankings without approximating exact distributions. Code is available at [anonymous repository].

2 Related Work

Causal reasoning in NLP has emerged as a central research direction. While traditional NLP focused on predictive tasks, current research explores extracting causal relationships from text. Feder et al. (2021) demonstrate that causal modeling improves NLP robustness and interpretability through intervention estimation from text. Text-based confounder identification has enabled more robust causal inference (Keith et al., 2020). Causal mining systematically extracts causal knowledge from text corpora (Ali et al., 2021; Yang et al., 2022), with applications in social science research (Ash & Hansen, 2023).

Language models now directly perform causal inference and discovery on linguistic representations (Wang et al., 2024). Researchers evaluate LMs on causal reasoning benchmarks designed to test these capabilities (Liu et al., 2024), and they can guide conventional causal discovery algorithms (Ban et al., 2023). LMs can perform causal reasoning in natural language processing and chain-of-thought tasks (Jin et al., 2024) as evaluated in benchmarks such as CaLM Chen et al. (2024). However, LMs struggle with counterfactual reasoning (Yang et al., 2024; Ashwani et al., 2024) and are sensitive to word order when doing causal inference (Joshi et al., 2024). Proposed solutions include specialized causal models, multimodal approaches, and unified benchmarks (Ma, 2024) while pre-trained LMs can enhance statistical causal discovery (Takayama et al., 2024), though commercial implementations exhibit limitations (Kıcıman et al., 2023).

Evidence suggests LMs discover causal models from data: Li et al. (2024a) showed GPT develops internal game representations when predicting Othello moves. Nanda et al. (2023) identified simpler linear representations that capture these emergent structures. Transformers encode latent belief states in their residual streams that guide next-token predictions (Shai et al., 2024).

3 Preliminaries

Causal modeling operates on random variables as its core mathematical objects. Let $(\Omega_1, \Sigma_1, \Pr)$ be a probability space and $(\mathbb{R}^n, \mathfrak{B}(\mathbb{R}^n))$ be a Borel measurable space of real-valued vectors. An n-dimensional *random vector* on $(\Omega_1, \Sigma_1, \Pr)$ is a Borel measurable map $X : \Omega_1 \to \mathbb{R}^n$ with components $X_i = p_i \circ X$, where $p_i : \mathbb{R}^n \to \mathbb{R}$ projects onto the ith coordinate. The probability function is $\Pr_X(X \in A) = \{w \in \Omega_1 : X(w) \in A\}$ for any $A \in \mathbb{R}^n$, with induced component probabilities $\Pr_{X_i} = \{\omega \in \Omega_1 : X_i(\omega) \in B\}$ for all $B \in \mathfrak{B}(\mathbb{R})$. The cumulative distribution function $F_X(\mathbf{x}) = \Pr_X(X_1 \leq x_1, \ldots, X_n \leq x_n)$ yields joint densities for continuous cases and mass functions for discrete cases. Causal discovery crucially relies on conditional independence relations between random variable sets. Two component sets $\mathbf{X}, \mathbf{Y}$ of random vector X are conditionally independent given $\mathbf{Z}$ if and only if $\Pr_{\mathbf{X}}(\mathbf{X}|\mathbf{Z}, \mathbf{Y}) = \Pr_{\mathbf{X}}(\mathbf{X}|\mathbf{Z})$.

Structural causal models (SCMs) are defined over random variable sets as follows:

Definition 3.1. A structural causal model M is a four-tuple $(\mathbf{U}, \mathbf{V}, \mathcal{F}, \Pr(u))$ where $\mathbf{U} = \{X_i \in X : i \in \{1, \ldots, n\}\}$ is a set of components from the random vector X of length n called the exogenous or unobserved variables, $\mathbf{V} = \{X_i \in X : X_i \notin \mathbf{U}\}$ is the complement of $\mathbf{U}$ in X called the endogenous or observed variables, $\mathcal{F} = \{f : U_i \cup pa_i \to V_i : i = 1, \ldots, n\}$ where $U_i \subseteq \mathbf{U}$ and $pa_i \subseteq \mathbf{V} - V_i$ is the set of functions mapping from parents in both the unobserved and observed variables to each member $V_i \in \mathbf{V}$, $\Pr(u)$ is the joint distribution for the components of X given in $\mathbf{U}$.

Each SCM partitions the random vector into observed and unobserved components, inducing a joint distribution over $\mathbf{V}$ through the unobserved distribution and functions in $\mathcal{F}$. The SCM induces a directed acyclic graph (DAG) G with vertices $\mathbf{V}$. This yields a correspondence between graph properties and conditional independencies: vertices are *d-separated* conditional on a third vertex based on three fundamental structures (chain, fork, collider), and d-separation equivalently characterizes conditional independence (Pearl (2009), Theorem 1.2.4).

Under certain assumptions, conditional independencies reveal structural causal model properties. Classic examples include Pearl (2009)'s IC/IC* and Spirtes et al. (2001)'s PC/PC* algorithms. These algorithms identify the smallest SCM equivalence class when the generating model satisfies Markov, Minimality, and Faithfulness conditions[1]:

Definition 3.2. An SCM M is *Markov* just in case the joint distribution of the observed component $\mathbf{V} = \{X_1, \ldots, X_m\}$ of our random vector for $m \leq n$ where pa is the parents of X_i in M:

$$\Pr_{\mathbf{V}}(X_1, \ldots, X_m) = \prod_{i=1}^{m} \Pr_{X_i}(X_i | pa(X_i)) \tag{1}$$

Definition 3.3. An SCM M satisfies *minimality* if and only if for every proper subgraph H of the SCM's DAG G defined on the observed variables $\mathbf{V}$ with a vertex set given by $\mathbf{V}$, the corresponding set of variables in that graph is not Markov on M's induced probability distribution.

Definition 3.4. An SCM M is *faithful* if its DAG G is such that any set of observed variables $\mathbf{X}, \mathbf{Y}, \mathbf{Z}$, the corresponding vertices for $\mathbf{X}$ is d-separated from $\mathbf{Y}$ by $\mathbf{Z}$ if and only if $\mathbf{X}$ is conditionally independent of $\mathbf{Y}$ given $\mathbf{Z}$ in M induced distribution Pr.

These conditions, plus *causal sufficiency* (no unobserved common causes) for some algorithms, enable recovery of the minimal partial DAG set (Pearl, 2009; Spirtes et al., 2001).

IC and PC algorithms have two limitations. First, they require exponential worst-case time for skeleton discovery (Le et al., 2016).[2] Second, they return only an equivalence class of DAGs that could have generated the data. Thus, these algorithms *underdetermine* the true causal model. Generally, probabilistic information alone cannot identify interventional relationships (Bareinboim et al., 2022). Additional assumptions are required for unique causal model identification.

4 A Theoretical Reason for Why LMs Can Do Causal Discovery

Completing a partial DAG requires orienting its undirected edges. This requires determining the correct interventional factorization: for neighbors X_1 and X_2 with an undirected edge, we must identify whether $\Pr(X_1 | do(X_2 = x)) = \Pr(X_1 | X_2 = x)$ or $\Pr(X_1 | do(X_2 = x)) = \Pr(X_1)$. Bareinboim et al. (2022) prove this is impossible from observational data alone (theorem 27.1). Additional assumptions enable causal discovery. Temporal ordering, if available, uniquely identifies the DAG structure of the generating SCM.

Definition 4.1. Let $M = (\mathbf{U}, \mathbf{V}, \mathcal{F}, \Pr(u))$ be a SCM. A temporal ordering of $(v_0, v_1, \ldots, v_n)$ on V is a total ordering such that for any $i < j$, v_i does not occur after v_j in time.

[1] While PC applications typically assume i.i.d. data (Glymour et al., 2019; Hasan et al., 2023), the algorithm only requires consistent statistical tests for distinguishing dependence from independence (Spirtes et al., 2001). Extensions exist for non-i.i.d. temporal data (Niu et al., 2024).

[2] Skeleton discovery in Bayes networks is NP-complete (Chickering, 1996).

Algorithm 1 Algorithm for causal discovery.

```
Apply PC or IC discovery algorithm
for all undirected edges between variables v_i, v_j do
    if i < j then
        Direct edge from v_i to v_j
    else
        Direct edge from v_j to v_i
    end if
end for
```

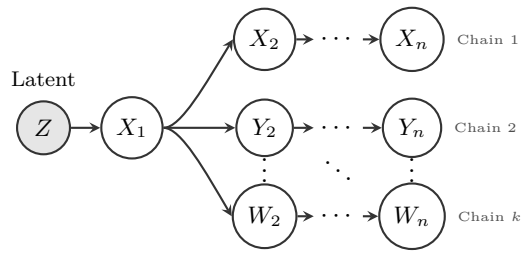

Figure 1: (Left) Algorithm for causal discovery. (Right) Causal model for Markov chain generation with k possible chains. The latent variable Z determines chain selection through initial token X_1. From X_1, the model generates k different sequences following distinct Markov dynamics, with vertical ellipses indicating chains 3 through $k-1$.

Algorithm 1 leverages temporal ordering to orient all edges in the CPDAG (Pearl (2009), chapter 3). This algorithm recovers the true DAG G under two conditions: causes precede effects temporally (Pearl (2009), definition 2.7.4) and unobserved variables have at most one child. This can be demonstrated in a straightforward proposition.

Proposition 4.2. *Let $M = (\mathbf{U}, \mathbf{V}, \mathcal{F}, \Pr(u))$ be a SCM with the corresponding DAG G of observed variables V and induced probability function* Pr*. Suppose M satisfies the Markov, faithfulness, and temporal ordering conditions and that for each $U \in \mathbf{U}$ has at most one child. Then there exists an algorithm for finding G.*

Thus, appropriate assumptions enable unique recovery of causal directions (as suggested by (Spirtes et al., 2001, p.93)). Two things should be noted. First, these minimal conditions may require augmented PC algorithms, for instance, require i.i.d. data for valid conditional independence tests. Second, real data may violate our assumptions through non-Markov processes, faithfulness violations, unobserved confounders, or missing temporal information.

Given this theoretical foundation, causal discovery requires two inductive biases: identifying appropriate probabilistic properties, e.g. conditional independencies and recognizing temporal order. Do LMs possess these biases?

LMs can identify temporal information through positional encodings, which transformers require due to their permutation invariance (Vaswani, 2017; Dufter et al., 2022). Absolute sinusoidal positional encoding adds the following to each sequence element's embedding (with dimension d):

$$\mathrm{PE}_{pos,k} = \begin{cases} \sin\left(\frac{pos}{10000^{k/d_{\text{model}}}}\right) & \text{if } k \text{ is even} \\ \cos\left(\frac{pos}{10000^{(k-1)/d_{\text{model}}}}\right) & \text{if } k \text{ is odd} \end{cases} \tag{2}$$

This enables transformers to track input order, thereby capturing temporal structure when present in the data.

Can LMs identify the probabilistic properties required for causal discovery? Lu & Lu (2020) demonstrate that ReLU networks can approximate arbitrary probability distributions to any Wasserstein-1 distance in the data limit. However, universal approximation does not guarantee that gradient descent finds these approximations on finite data (except potentially when overparameterized with infinite data (Rotskoff & Vanden-Eijnden, 2018)). Empirical testing must verify whether transformers learn the requisite probabilistic properties.

We test whether generative models learn correct conditional independencies. However, our experiments reveal that conditional independence alone insufficiently evaluates LMs' causal discovery capabilities. Prob-

abilistic symmetry properties provide an alternative evaluation. In the Bayesian interpretation, probabilities represent an agent's degrees of belief rather than external facts. Causal discovery then becomes identifying which mixture of causal models the agent's probabilities encode. De Finetti's theorem states that exchangeable (permutation-invariant) Bernoulli sequences admit representation as mixtures over i.i.d. distributions conditioned on a latent variable (Kirsch, 2019). Importantly, pre-trained LMs appear to demonstrate these symmetry properties in-context (Zhang et al., 2023; Falck et al., 2025). If LMs learn exchangeability, causal discovery reduces to identifying the correct mixture component—effectively detecting conditional independencies without explicit latent variable search.

Exchangeability generalizes to Markov exchangeability. The *transition count matrix* for a discrete random vector with n states records transitions between values $i = 0, 1, \ldots, n$:

$$\begin{pmatrix} a_{00} & a_{01} & \ldots & a_{0n} \\ a_{10} & a_{11} & \ldots & a_{1n} \\ \vdots & \vdots & \ddots & \vdots \\ a_{n0} & a_{n1} & \ldots & a_{nn} \end{pmatrix} \tag{3}$$

where each a_{ij} is the transition counts from values i to j. We can then define Markov exchangeability:

Definition 4.3. Let $\Pr_X$ be a probability function defined on the random vector $X = [X_1, \ldots, X_n]$ and let $\rho \mapsto j \neq i$ for $i, j \in \mathbb{N}/\{1\}$ be any permutation that maps the i-th component to the j-th component such that the resulting random vector has the same 1-st component and transition matrix as X. $\Pr_X$ is *Markov exchangeable* if:

$$\Pr_X(X_{\rho(1)} = x_1, \ldots, X_{\rho(n)} = x_n) = \Pr_X(X_1 = x_1, \ldots, X_n = x_n) \tag{4}$$

For recurrent processes (where some state $x \in S$ satisfies $\Pr_X(X_i = x \text{ infinitely often}) = 1$), Diaconis & Freedman (1980) prove that Markov exchangeable distributions are *uniquely* representable as Markov chain mixtures (theorem 22).

Therefore, we can use the symmetry property of Markov exchangeability as an additional test to identify when probabilistic models have learned *some* mixture of Markov chains. It is an orthogonal property to conditional independence that can be used to identify when LM probabilities encode the right kind of graphical structure without specifying the exact Markov processes involved.

5 Experiments

In this section, we document our experimental methods and results. We describe our synthetic datasets and model architectures, then report results for three experiments: conditional independence tests, probabilistic symmetry tests, and distribution approximation analyses.

5.1 Experimental Methods and Procedures

We use synthetic data for two reasons: real-world datasets lack known generating models, and synthetic data provides a best-case scenario for testing language models. Synthetic data provides three advantages. It allows experimental control over the generating distribution, precise evaluation through direct comparison with ground truth, and generalizability to any discrete sequential dataset. We use a mixture of Markov processes, one of the simplest causal models satisfying both proposition 4.2 and the Markov exchangeability conditions from definition 4.3. Figure 1 shows this model's causal structure.

Each dataset consists of sequences with categorical values $i \in \{0, 1, 2, 3, 4, 5\}$. We generate each sequence by first sampling from a prior distribution $\Pr(X_1)$, which determines the stochastic matrix governing subsequent tokens (see appendix B for examples). Once set, we sample from this matrix to generate the remaining tokens and record each sequence's log probability. We test sequence lengths of 6, 100, and 500 tokens,

	$\mathbf{X_{i-1} = 1}$	$\mathbf{X_{i-1} = 2}$	$\mathbf{X_{i-1} = 3}$	$\mathbf{X_{i-1} = 4}$	$\mathbf{X_{i-1} = 5}$	$\mathbf{X_{i-1} = 6}$
χ^2 **P-value**	0.028	0.023	<0.001	0.025	0.003	<0.001
Observed Cramer's V	0.067	0.051	0.033	0.065	0.046	0.030

Table 1: Baseline Chi-Squared Tests: Columns indicate $X_{i-1} = k$ for $k \in \{1, \ldots, 6\}$. Tests check whether the i-th variable is conditionally independent of all $j > i-1$ variables given the $(i-1)$-th and 0-th variables. Rows show average p-values (null: variables dependent, threshold $V = 0.15$) and observed Cramer's V. Results from $N = 100{,}000$ i.i.d. sequences; all standard deviations ≈ 0.00.

training separate models for each length. We report results for 100-token sequences; results for 6- and 500-token sequences were identical. Dataset sizes ranged from 62,500 to 6,250,000 sequences, selected to match Chinchilla-optimal token counts for our model parameters (Hoffmann et al., 2022). We split all datasets 80/20 into training and validation sets. By construction, the data distribution is Markov, minimal, and faithful.

We evaluate four architectures: Neural Autoregressive Distribution Estimator (NADE) (Uria et al., 2016), Encoder-Decoder transformer (Vaswani, 2017), Decoder-only transformer (Radford, 2018), and Switch transformer (Fedus et al., 2022; Shazeer et al., 2017). Appendix C details architecture specifications and selection criteria. After hyperparameter selection and training, we conducted the experiments described below.

5.2 Identifying Conditional Independence

Our first experiment tests whether models learn the data's conditional independence structure. Since we generated each dataset via a component in a mixture of Markov processes, each token's conditional probability depends only on its immediate predecessor and the initial token, which implies equality between that conditional probability and the token conditional on all tokens that came previously. We test whether models learn this conditional independence:

$$\Pr_m(X_i = x_i | X_{i-1} = x_{i-1}, \ldots, X_1 = x_1) = \Pr_m(X_i = x_i | X_{i-1} = x_{i-1}, X_1 = x_1) \tag{5}$$

As a baseline for checking whether PC would identify the mixture-of-Markov chains structure, we run χ^2 equivalence tests on randomly drawn sequences from a training dataset. This checks for conditional independence against the equivalence null that they are dependent. Table 1 reports the average p-values and observed Cramer's V. We find that sequences are conditionally independent as warranted by equation 5.

To assess whether models learn this Markov property, we test the conditional independence in Equation 5. We measured the similarity between these distributions using the Jensen-Shannon Divergence (JSD); JSD ranges from 0 (identical distributions) to 1 (maximally difference).[3] For each position i in a sequence, we obtain two distributions from the model m through separate forward passes. The first uses full context $X_{i-1}, \ldots, X_1$ to predict X_i; the second uses only X_{i-1}, X_1. We then compute the JSD between these distributions. We test both trained and randomly initialized models.

Table 2a shows these results. The 95% confidence intervals for trained transformers' mean JSD are close to but above zero. An independent-samples t-test (80% power) confirms that trained models' JSD significantly differs from random initialization. This indicates that training induces partial learning of conditional independence structure, though not perfect adherence to the Markov property. Furthermore, we observe that non-trained model exhibit near-0 JSD means. This occurs because the random Xavier initialization produces weight distributions that render the model's predictions approximately independent of the input context. Since both conditional distributions $\Pr_m(X_i | X_{i-1}, X_1)$ and $\Pr_m(X_i | X_{i-1}, \ldots, X_1)$ are approximately independent of their conditioning sets, they trivially match each other, which yields low JSD. We therefore conduct additional symmetry tests (section 5.3) to better characterize what models learn.

[3] Our conditional independence test does not require i.i.d. data. Both our generated data and the generative models learning from it are explicitly non-i.i.d. Traditional tests would fail in this setting, but the causal discovery requirements from Proposition 4.2 are still satisfied when a model can learn the necessary conditional independence structures.

Model	JSD-Train 0.95 CI	JSD-NT μ
NADE	(0.004, 0.031)	0.002
Enc.-Dec.-T.	(0.072, 0.255)	0.037
Decoder-T.	(0.113, 0.407)	0.042
Switch-T.	(0.151, 0.451)	0.037

(a) Markov Property Tests: The Jensen-Shannon Divergence (JSD) assesses if models learn the Markov property as defined in Eq. 5; a value closer to 0 indicates a better fit. The table shows 95% confidence intervals (CI) for trained models and the mean JSD for non-trained models. JSD tests used $N = 6388$.

Model	Train CI μ	No-train CI μ
Enc.-Dec.-T.	(3.00, 3.14)	(-5.75, -5.59)
Decoder-T.	(3.19, 3.32)	(-6.21, -6.02)
Switch-T.	(3.98, 4.13)	(-5.60, -5.42)

(b) Log Probability Differences: The mean log probability difference between a model's assigned probability and the true probability for a sequence; a value closer to 0 indicates better distribution approximation. The table shows 95% confidence intervals (CI) for both trained and non-trained models. Log probability tests used $N = 1598$.

Table 2: Comparison of model performance metrics.

5.3 Symmetry Property Experiments

Since conditional independence tests cannot discriminate trained from untrained models, we test Markov exchangeability to determine whether models learn the mixture-of-Markov-processes structure. We measure the probability ratio between a sequence $X_1, \ldots, X_n$ and its Markov-exchangeable permutation $X_{\rho(1)}, \ldots, X_{\rho(n)}$. For numerical stability, we use log probabilities, converting the ratio to a difference: $\log \Pr_m(X_1, \ldots, X_n) - \log \Pr_m(X_{\rho(1)}, \ldots, X_{\rho(n)})$. Values near 0 indicate nearly identical probabilities. We compute model joint probabilities using the autoregressive factorization: $\log \Pr_m(X_1, \ldots, X_n) = \sum_{i=1}^{n} \log \Pr_m(X_i | X_1, \ldots, X_{i-1})$ where we obtain each conditional probability from the model's softmax output for position i with the $1, \ldots, i-1$ input context. We hypothesize that trained models exhibit two properties: (1) mean log differences near 0 for Markov-exchangeable permutations, and (2) variance below 1.0 (indicating concentration). These properties should fail for random sequence pairs. We conjecture that training induces these properties, which randomly initialized models lack.

Our experimental procedure consists of five steps: (1) sample $N = 1598$ sequences from the train/test split; (2) for each sequence, generate 3 Markov-exchangeable permutations and select 3 random sequences from both the training and test distribution; (3) compute model log probabilities for all sequences, permutations, and random samples; (4) calculate log probability differences between the target sequence and its permutations and random samples; (5) average differences across permutations and random samples.

We conduct frequentist and Bayesian equivalence tests with bounds $[x_{lower}, x_{higher}] \in \{[-1.0, 1.0], [-0.5, 0.5], [-0.1, 0.1]\}$. We reject the null hypotheses $\mu_0 > x_{higher}$ or $\mu_0 < x_{lower}$ when the mean falls within the bounds. For variance, we test $\sigma_0^2 > 1.0$, where rejection indicates concentration around 0. We compute 95% confidence intervals and Bayesian credible/highest density intervals (details in appendix D). Figure 2 shows the results. All models except the Decoder-only Transformer reject the null hypothesis at all thresholds (circles in Figure 2a). However, comparing sequences to random samples fails to reject the null at the $[-0.1, 0.1]$ threshold (stars in Figure 2a). For variance tests, all models except NADE reject the null for Markov-exchangeable permutations (circles in Figure 2b) but not for random sequences (stars), with large effect sizes. These results indicate that Encoder-Decoder and Switch Transformers learn Markov exchangeability, the Decoder-only Transformer partially learns it, and NADE does not.

Our second hypothesis posits that training induces Markov exchangeability rather than it emerging from random initialization of the architecture alone. We compare trained and randomly initialized models. All non-trained models were initialized as is standard with Xavier distributions on the weights. Figure 2 presents these comparisons. For randomly initialized models (Figure 2c), NADE shows results identical to trained models, while other architectures fail the strictest null hypothesis test ($[-0.1, 0.1]$), which provides weak evidence that non-NADE architectures exhibit some inherent Markov exchangeability. Variance analysis reveals stark differences (Figure 2d): randomly initialized models (except NADE) show significantly higher variances that fail to reject the null hypothesis. This confirms that training induces partial learning of the mixture-of-

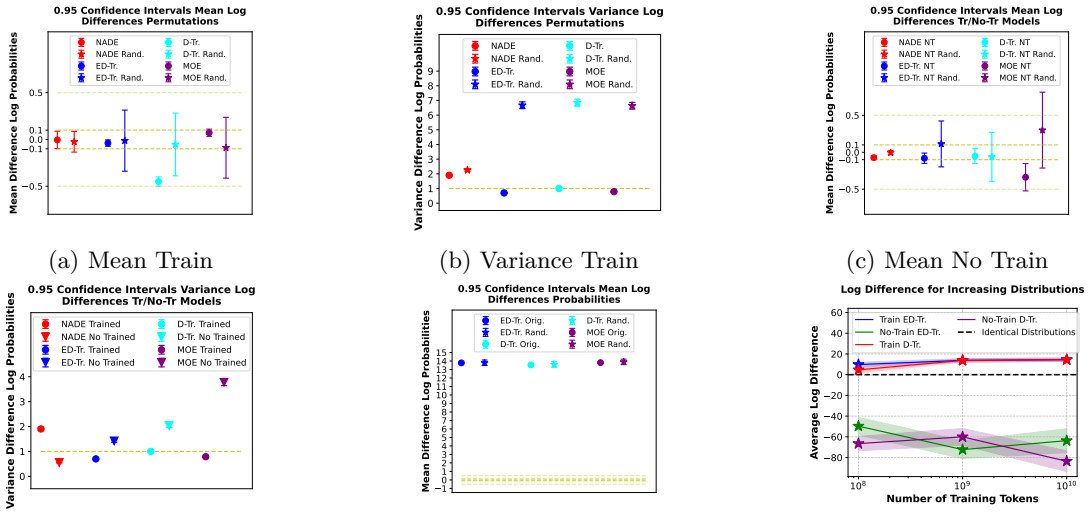

(a) Mean Train (b) Variance Train (c) Mean No Train

(d) Variance No Train (e) Gap between distributions (f) Increasing Differences

Figure 2: Confidence intervals (0.95) for: (a-b) Mean and variance of log differences between sequences and permutations; (c-d) Comparison between trained vs. non-trained models; (e) Gap between model and true probability assignments; (f) Impact of training data volume on model confidence. Dashed lines indicate null hypothesis thresholds

Markov-chains structure for all models except NADE, consistent with the conditional independence results (section 5.2).

5.4 Learning by Approximating the Underlying Distribution

One hypothesis for the observed learning is that models approximate the true data distribution, correctly estimating sequence probabilities. Universal approximation theorems for feedforward networks with ReLU activations (Lu & Lu, 2020) support this possibility.

Our synthetic data enables exact computation of each sequence's $X_1, \ldots, X_n$ true probability from the prior and transition matrices. We measure distribution approximation as the log probability difference between the model's distribution and the true distribution: $\log \Pr_m(X_1, \ldots, X_n) - \log \Pr_{dist}(X_1, \ldots, X_n)$. As a baseline, we also compare model probabilities for random sequences against the true probabilities of X. We apply the same statistical tests as in section 5.3. We also compute Wasserstein-1 distances, but all values are near zero, including for random sequences. We therefore omit these uninformative results.

Figure 2e shows 95% confidence intervals for mean differences across $N = 1598$ samples, relative to our null hypotheses. All architectures assign significantly higher probabilities than ground truth—not only to original sequences but also to random sequences, leading us to reject the distribution approximation hypothesis.

We next investigate whether overconfidence stems from insufficient data exposure. Training data represents a tiny fraction of the space; the overall number of possible sequences that could be observed (6.25×10^7 training sequence compared to 6.53×10^{77} possible sequences). We conduct two experiments to test this. First, we vary training data size across multiple orders of magnitude. If limited data causes overconfidence, models should assign probabilities closer to ground truth as dataset size increases. Memory constraints limit this experiment to Encoder-Decoder and Decoder-only transformers ($N = 1598$ sequences). Second, we create a length-6 dataset containing 46,656 possible sequences and densely sample 500,000 training sequences. With exposure to most possible sequences, models should memorize exact probabilities if overconfidence results from limited data.

Figure 2f shows the first experiment's results. Counterintuitively, log probability gaps *increase* with more training data even as the relative order of magnitude of the number of tokens increases. This means that the

Model	Similarity T	Similarity NT	Levenshtein T	Levenshtein NT
Enc.-Dec.-T.	0.55	0.45	0.31	0.24
Decoder-T.	0.55	0.53	0.31	0.29
Switch.-T	0.55	0.48	0.31	0.23
Random Assignment	0.02	0.02	0.01	0.01

Table 3: Similarity metrics between model probability rankings and ground truth (T=Trained, NT=Non-Trained). Higher values indicate greater similarity to transition matrices. All models significantly outperform random baselines.

models grow more confident about the probabilities as it sees more data. To verify this is not an architectural artifact, we examine randomly initialized models. Untrained models show the opposite pattern of slightly decreasing confidence as dataset size increases

Table 2b presents the second experiment's results. Even with near-complete data coverage, all models assign probabilities significantly above ground truth, exhibiting systematic overconfidence. This definitively rules out distribution approximation as the learning mechanism.

Given that models do not learn exact probabilities, we test whether they learn *qualitative rankings*. We examine how models rank token probabilities at each position in 100-token sequences. For $N = 1598$ sequences, we compare model rankings to the true transition matrix. Table 3 shows mean similarity scores. We compute two metrics: a pairwise ranking similarity (appendix D) and Levenshtein distance with substitution costs. Trained models show substantially higher ranking similarity than both random baselines and untrained models, except for the Decoder-only Transformer. This shows that the models learn ordinal structure—correct relative rankings—while failing to learn cardinal structure, i.e. correct absolute probabilities.

6 Discussion

Prior work on causal discovery with LMs utilizes LMs to extract causal relationships *represented* in text, such as identifying whether smoking causes cancer from medical literature. Similarly, applications of LMs to causal inference estimate causal effects using token-level representations of observed variables. We address a more fundamental question: can LMs discover the causal processes that *generate* token sequences?

Token-level causal learning could support semantic understanding in at least two cases. First, when causal relationships in text are consistently expressed in temporal directly in text, e.g. "X happened, then Y, which caused Z". Semantic causal relationships can then be extracted from token causal relationships. Second, the token generation process reflects the author's causal model of the domain, e.g. there are latent variables explaining the sequential ordering such as the transition matrices used in our experiments. Our results show that LMs possess the necessary inductive biases for token-level causal discovery. Verifying whether both of these cases are viable for semantic understanding remains an open empirical question.

Understanding LM inductive biases for causal discovery is critical because traditional methods scale poorly to high-dimensional token spaces. Constraint-based methods (e.g., PC, FCI), score-based methods (e.g., GES), and functional causal models (e.g., LiNGAM) offer sound theoretical guarantees but scale poorly with dimensionality. In contrast, LMs learn compressed representations of high-dimensional distributions, enabling tractable causal discovery when their inductive biases align with causal structure. LMs offer an additional advantage: while traditional methods require i.i.d. observations, LMs require only that training sequences are sampled i.i.d., not that tokens are independent. This relaxed assumption enables causal discovery on sequential data with inherently dependent observations, such as natural language corpora.

Our experiments demonstrate that LMs possess appropriate inductive biases for causal discovery on temporally ordered data. Theoretically, Proposition 4.2 establishes that unique causal discovery on temporal data requires both identifying probabilistic symmetries and leveraging temporal order. Positional encoders, standard in LM architectures, naturally provide temporal ordering information. Our experiments show that LMs learn to identify these probabilistic symmetries. Models identify these symmetries through ordinal

probability rankings rather than accurate distributional approximation. We hypothesize this behavior stems from systematic overconfidence in transformer architectures and training procedures, a well-documented phenomenon (Guo et al., 2017; Wei et al., 2022). While LMs show promise for causal discovery, their capacity for accurate causal effect estimation may be severely limited.

Our results inform ongoing debates about whether LMs can perform causal reasoning. These debates focus on reasoning about causal variables *represented* or *described* in text. A prerequisite question is whether LMs can learn representations of the causal processes generating their training data. While initial work suggested LMs learn coherent world models (Li et al., 2024a), subsequent experiments found they learn incoherent physical rules (Vafa et al., 2025). This literature could benefit from applying formal causal models from causal inference and discovery. Our experiments suggest that LMs can learn representations by discovering the causal processes generating their training data. However, systematic overconfidence may bias LMs toward learning only ordinal rankings, indicating reliance on heuristics rather than principled probabilistic inference. Improved calibration to the true data-generating distribution may therefore reduce this bias toward improper representations.

Limitations: Our conclusions have several important limitations. First, our experiments address identifying the processes that generate tokens, not extracting causal relationships described in text. Second, our results assume Markov, minimal, and faithful distributions with temporal ordering and no unobserved confounders. Most traditional causal discovery applications involve unordered tabular data without natural temporal structure. Whether LMs retain these inductive biases for non-sequential data remains open. Third, while LMs learn qualitative probability rankings sufficient for causal discovery, this may impair causal effect estimation. Fourth, our experiments use synthetic data from first-order Markov processes rather than naturalistic text corpora. Validating these findings on natural language data is essential future work.

References

Wajid Ali, Wanli Zuo, Rahman Ali, Xianglin Zuo, and Gohar Rahman. Causality mining in natural languages using machine and deep learning techniques: A survey. *Applied Sciences*, 2021. URL https://api.semanticscholar.org/CorpusID:240165843.

Elliott Ash and Stephen Hansen. Text algorithms in economics. *Annual Review of Economics*, 15(1):659–688, 2023.

Swagata Ashwani, Kshiteesh Hegde, Nishith Reddy Mannuru, Mayank Jindal, Dushyant Singh Sengar, Krishna Chaitanya Rao Kathala, Dishant Banga, Vinija Jain, and Aman Chadha. Cause and effect: Can large language models truly understand causality?, 2024. URL https://arxiv.org/abs/2402.18139.

Taiyu Ban, Lyvzhou Chen, Xiangyu Wang, and Huanhuan Chen. From query tools to causal architects: Harnessing large language models for advanced causal discovery from data, 2023. URL https://arxiv.org/abs/2306.16902.

Elias Bareinboim, Juan D Correa, Duligur Ibeling, and Thomas Icard. On pearl's hierarchy and the foundations of causal inference. In *Probabilistic and causal inference: the works of Judea Pearl*, pp. 507–556. ACM, 2022.

Sirui Chen, Bo Peng, Meiqi Chen, Ruiqi Wang, Mengying Xu, Xingyu Zeng, Rui Zhao, Shengjie Zhao, Yu Qiao, and Chaochao Lu. Causal evaluation of language models, 2024. URL https://arxiv.org/abs/2405.00622.

David Maxwell Chickering. Learning bayesian networks is np-complete. In *Learning from data: Artificial intelligence and statistics V*, pp. 121–130. Springer, 1996.

Persi Diaconis and David Freedman. de finetti's theorem for markov chains. *The Annals of Probability*, pp. 115–130, 1980.

Philipp Dufter, Martin Schmitt, and Hinrich Schütze. Position information in transformers: An overview. *Computational Linguistics*, 48(3):733–763, 2022.

Fabian Falck, Ziyu Wang, and Chris Holmes. Is in-context learning in large language models bayesian? a martingale perspective. In *Proceedings of the 41st International Conference on Machine Learning*, ICML'24. JMLR.org, 2025.

Amir Feder, Katherine A. Keith, Emaad A. Manzoor, Reid Pryzant, Dhanya Sridhar, Zach Wood-Doughty, Jacob Eisenstein, Justin Grimmer, Roi Reichart, Margaret E. Roberts, Brandon M Stewart, Victor Veitch, and Diyi Yang. Causal inference in natural language processing: Estimation, prediction, interpretation and beyond. *Transactions of the Association for Computational Linguistics*, 10:1138–1158, 2021. URL https://api.semanticscholar.org/CorpusID:237386009.

William Fedus, Barret Zoph, and Noam Shazeer. Switch transformers: Scaling to trillion parameter models with simple and efficient sparsity. *Journal of Machine Learning Research*, 23(120):1–39, 2022.

Clark Glymour, Kun Zhang, and Peter Spirtes. Review of causal discovery methods based on graphical models. *Frontiers in genetics*, 10:524, 2019.

Chuan Guo, Geoff Pleiss, Yu Sun, and Kilian Q Weinberger. On calibration of modern neural networks. In *International conference on machine learning*, pp. 1321–1330. PMLR, 2017.

Gyandev Gupta, Bashir Rastegarpanah, Amalendu Iyer, Joshua Rubin, and Krishnaram Kenthapadi. Measuring distributional shifts in text: The advantage of language model-based embeddings, 2023. URL https://arxiv.org/abs/2312.02337.

Uzma Hasan, Emam Hossain, and Md Osman Gani. A survey on causal discovery methods for i.i.d. and time series data. *Transactions on Machine Learning Research*, 2023. ISSN 2835-8856. URL https://openreview.net/forum?id=YdMrdhGx9y. Survey Certification.

Jordan Hoffmann, Sebastian Borgeaud, Arthur Mensch, Elena Buchatskaya, Trevor Cai, Eliza Rutherford, Diego de Las Casas, Lisa Anne Hendricks, Johannes Welbl, Aidan Clark, et al. Training compute-optimal large language models. *arXiv preprint arXiv:2203.15556*, 2022.

Zhijing Jin, Yuen Chen, Felix Leeb, Luigi Gresele, Ojasv Kamal, Zhiheng Lyu, Kevin Blin, Fernando Gonzalez Adauto, Max Kleiman-Weiner, Mrinmaya Sachan, and Bernhard Schölkopf. Cladder: Assessing causal reasoning in language models, 2024. URL https://arxiv.org/abs/2312.04350.

Nitish Joshi, Abulhair Saparov, Yixin Wang, and He He. Llms are prone to fallacies in causal inference. *arXiv preprint arXiv:2406.12158*, 2024.

Katherine A. Keith, David D. Jensen, and Brendan T. O'Connor. Text and causal inference: A review of using text to remove confounding from causal estimates. *ArXiv*, abs/2005.00649, 2020. URL https://api.semanticscholar.org/CorpusID:218487374.

Emre Kıcıman, Robert Ness, Amit Sharma, and Chenhao Tan. Causal reasoning and large language models: Opening a new frontier for causality. *arXiv preprint arXiv:2305.00050*, 2023.

Werner Kirsch. An elementary proof of de finetti's theorem. *Statistics & Probability Letters*, 151:84–88, 2019.

Thuc Duy Le, Tao Hoang, Jiuyong Li, Lin Liu, Huawen Liu, and Shu Hu. A fast pc algorithm for high dimensional causal discovery with multi-core pcs. *IEEE/ACM transactions on computational biology and bioinformatics*, 16(5):1483–1495, 2016.

Kenneth Li, Aspen K. Hopkins, David Bau, Fernanda Viégas, Hanspeter Pfister, and Martin Wattenberg. Emergent world representations: Exploring a sequence model trained on a synthetic task, 2024a. URL https://arxiv.org/abs/2210.13382.

Yufei Li, Simin Chen, Yanghong Guo, Wei Yang, Yue Dong, and Cong Liu. Uncertainty awareness of large language models under code distribution shifts: A benchmark study, 2024b. URL https://arxiv.org/abs/2402.05939.

Xiaoyu Liu, Paiheng Xu, Junda Wu, Jiaxin Yuan, Yifan Yang, Yuhang Zhou, Fuxiao Liu, Tianrui Guan, Haoliang Wang, Tong Yu, Julian McAuley, Wei Ai, and Furong Huang. Large language models and causal inference in collaboration: A comprehensive survey. *ArXiv*, abs/2403.09606, 2024. URL https://api.semanticscholar.org/CorpusID:268385564.

Yulong Lu and Jianfeng Lu. A universal approximation theorem of deep neural networks for expressing probability distributions. *Advances in neural information processing systems*, 33:3094–3105, 2020.

Jing Ma. Causal inference with large language model: A survey, 2024. URL https://arxiv.org/abs/2409.09822.

Neel Nanda, Andrew Lee, and Martin Wattenberg. Emergent linear representations in world models of self-supervised sequence models, 2023. URL https://arxiv.org/abs/2309.00941.

Wenjin Niu, Zijun Gao, Liyan Song, and Lingbo Li. Comprehensive review and empirical evaluation of causal discovery algorithms for numerical data, 2024. URL https://arxiv.org/abs/2407.13054.

J Pearl. *Causality.* Cambridge University Press, 2009.

Alec Radford. Improving language understanding by generative pre-training. *OpenAI Technical Report*, 2018.

Grant M Rotskoff and Eric Vanden-Eijnden. Neural networks as interacting particle systems: Asymptotic convexity of the loss landscape and universal scaling of the approximation error. *stat*, 1050:22, 2018.

Adam S. Shai, Sarah E. Marzen, Lucas Teixeira, Alexander Gietelink Oldenziel, and Paul M. Riechers. Transformers represent belief state geometry in their residual stream, 2024. URL https://arxiv.org/abs/2405.15943.

Noam Shazeer, Azalia Mirhoseini, Krzysztof Maziarz, Andy Davis, Quoc Le, Geoffrey Hinton, and Jeff Dean. Outrageously large neural networks: The sparsely-gated mixture-of-experts layer. *arXiv preprint arXiv:1701.06538*, 2017.

Peter Spirtes, Clark Glymour, and Richard Scheines. *Causation, prediction, and search.* MIT press, 2001.

Masayuki Takayama, Tadahisa Okuda, Thong Pham, Tatsuyoshi Ikenoue, Shingo Fukuma, Shohei Shimizu, and Akiyoshi Sannai. Integrating large language models in causal discovery: A statistical causal approach. *arXiv preprint arXiv:2402.01454*, 2024.

Benigno Uria, Marc-Alexandre Côté, Karol Gregor, Iain Murray, and Hugo Larochelle. Neural autoregressive distribution estimation. *Journal of Machine Learning Research*, 17(205):1–37, 2016.

Keyon Vafa, Peter G Chang, Ashesh Rambachan, and Sendhil Mullainathan. What has a foundation model found? using inductive bias to probe for world models. *arXiv preprint arXiv:2507.06952*, 2025.

A Vaswani. Attention is all you need. *Advances in Neural Information Processing Systems*, 2017.

Zhijing Wang, Yunhao Long, Zhijing Jin, et al. Large language models for causal discovery: Current landscape and future directions. *arXiv preprint arXiv:2402.11068*, 2024.

Hongxin Wei, Renchunzi Xie, Hao Cheng, Lei Feng, Bo An, and Yixuan Li. Mitigating neural network overconfidence with logit normalization. In *International conference on machine learning*, pp. 23631–23644. PMLR, 2022.

Jie Yang, Jiawei Huang, Jiming Ni, et al. A survey on extraction of causal relations from natural language text. *Knowledge and Information Systems*, 64(5):1161–1199, 2022.

Linying Yang, Vik Shirvaikar, Oscar Clivio, and Fabian Falck. A critical review of causal reasoning benchmarks for large language models, 2024. URL https://arxiv.org/abs/2407.08029.

Liyi Zhang, R. Thomas McCoy, Theodore R. Sumers, Jian-Qiao Zhu, and Thomas L. Griffiths. Deep de finetti: Recovering topic distributions from large language models. *ArXiv*, abs/2312.14226, 2023. URL `https://api.semanticscholar.org/CorpusID:266521340`.

Lin Zhu, Weihan Yin, Yiyao Yang, Fan Wu, Zhaoyu Zeng, Qinying Gu, Xinbing Wang, Chenghu Zhou, and Nanyang Ye. Vision-language alignment learning under affinity and divergence principles for few-shot out-of-distribution generalization. *Int. J. Comput. Vision*, 132(9):3375–3407, mar 2024. ISSN 0920-5691. doi: 10.1007/s11263-024-02036-4. URL `https://doi.org/10.1007/s11263-024-02036-4`.

A Proof of Proposition 4.2

We claim the algorithm in 1 will produce G. Since M is Markov and faithful, then the PC or IC algorithm will produce the Markov equivalence class of G, which is represented in the completed CPDAG, H. We then show that applying the algorithm will produce G by induction.

Base case: consider all neighbors of v_0. Any edges involving v_0 must be directed away since in H, any neighbors will be undirected or away due to colliders, while any additional undirected neighbors will have been oriented away due to the temporal ordering, which respects causation and so will be respected in G.

Inductive case: suppose that for variables $(v_0, \ldots, v_{n-1})$, the edges are oriented correctly in as in G. Consider variable v_n. For any neighbor v_i, either $i < n$ or $i > n$. If $i < n$, then by hypothesis the edges are oriented correctly in G. If $i > n$, then the algorithm will have oriented them from v_n to v_i, which will be respected in G since v_n occurs before v_i.

B Example Priors and Stochastic Matrices

Starting Token	**Prior**
0	0.061742605
1	0.10922861
2	0.287429074
3	0.063535748
4	0.141853226
5	0.336210737

Table 4: Sample priors for the 100-length dataset used on the Encoder-Decoder Transformer. Prior probabilities were taken from a normalized uniform distribution $\mathcal{U}(0, 1)$. Each probability corresponds to the probability of the first token in the sequence, which then has a corresponding stochastic matrix.

	0	1	2	3	4	5
0	0.234312928	0.27023688	0.00602517	0.22205389	0.207990725	0.059380408
1	0.054615949	0.248166706	0.113736672	0.246896763	0.197805355	0.138778555
2	0.322262131	0.293188673	0.12449644	0.01518472	0.106163398	0.138704637
3	0.17178788	0.242553914	0.086731108	0.185821451	0.144548306	0.168557341
4	0.065308119	0.172370142	0.104083311	0.148420859	0.221742868	0.288074701
5	0.040421359	0.04995777	0.12288811	0.252494683	0.323080174	0.211157903

Table 5: Sample recurrent stochastic matrix for the prior token 2 in table 4. This matrix was used to produce all of the sequences that the Encoder-Decoder Transformer architecture was trained and tested on. The matrix was generated by sampling each row from a uniform probability distribution $\mathcal{U}(0, 1)$ and then renormalized.

C Details on Training and Architectures

For selecting our model architecture, we performed pairwise grid search on the following parameters with 10-fold cross-validation on a small dataset of 60000 100-length sequences trained on each fold for 25 epochs. For learning rates, we tested $[0.1, 0.01, 0.001, 0.0001, 0.00001]$; for the NADE, we tested $[8, 16, 32, 64, 128, 256, 512, 1024, 2048, 4096]$ hidden units; for the various transformer architectures, we tested $[2, 5, 10]$ heads, $[2, 4, 6, 8, 10, 12]$ encoder and decoder layers, dropout probabilities of $[0.0, 0.1, 0.2, 0.3, 0.4]$, feedforward networks with $[8, 16, 32, 64, 128, 256, 512, 1024, 2048, 4096]$ hidden units; for the switch transformer, we also tested $[2, 3, 4, 5, 6]$ experts with the top 2 experts. The corresponding NADE, Encoder-Decoder transformer, Decoder-only transformer, and Switch transformer architectures found to have the lowest cross-validation losses are given in table 6. Note that for the Switch transformer, we used a decoder-only Switch transformer. For our short sequence tests, we used sequences of length 6. This required us to revise our architectures slightly by changing the number of heads to 6 for all architectures.

Model	**LR**	**FF**	**Heads**	**Enc. Lyrs**	**Dec. Lyrs**	**Dropout**	**Experts**
NADE	0.0001	16	NA	NA	NA	NA	NA
Transformer	0.0001	2048	5	2	8	0.0	NA
Dec. Trans.	0.0001	4096	10	NA	4	0.0	NA
Switch Trans.	0.0001	4096	10	NA	4	0.0	5

Table 6: The various architectures we used in our primary training experiments, selected via grid search and 10-fold cross-validation.

Once selected, all models were trained on their respective training datasets using the Adam optimizer with a cosine annealing learning rate scheduler for the transformers and a step scheduler for the NADE. The NADE was trained for 250 epochs with each mini-batch being 100 samples, with the learning rate halved every 50 epochs. The Encoder-Decoder and Decoder-only transformers were trained for 4 epochs with each mini-batch being 250 samples; the Switch transformer was trained for only 2 epochs with each mini-batch being 100 samples. Models were assessed on validation set drawn 80/20 from the training distribution. We observed during training that all models showed continual decreases in training and validation loss.

D Statistical Methods

For our symmetry experiments, we ran equivalence tests and computed confidence intervals, credibility intervals, and highest density intervals for the averages. Our equivalence tests consisted of two, one-sided t-tests to define our null hypotheses. Our alternatives were $(-1.0, 1.0)$, $(-0.5, 0.5)$, $(-0.25, 0.25)$, and $(-0.1, 0.1)$, which correspond to the models' having between 0.36 times smaller or 1.7 times greater probabilities, 0.61 times smaller or 0.64 times greater probabilities, 0.78 times smaller or 0.28 times greater probabilities, 0.90 times smaller or 0.10 times greater probabilities assigned to the original sequence compared to Markov exchangeable permutations. This effectively bounds the relative ratio of probabilities within $2, 1, 0.5$, and 0.2. Each one-sided t-test checked the null hypothesis below or above the bound, depending on the side. For the variances, we used a one-side t-test with the null $\sigma^2 > 1.0$ and the alternative being $\sigma^2 \leq 1.0$. We ran a chi-square test against the null and computing the 0.95 confidence intervals. Credibility and highest density intervals were computed concerning the prior $\mathcal{N}(0, 10)$, which we chose to ensure a good enough spread of possible values outside of the standard normal range. All tests unless otherwise noted were run with $N = 1598$ samples for 80% power for an effect size of 0.1. We estimated the population variance on a trial dataset, found it to be roughly 1, and then computed at $\beta = 0.2$ with an effect size of 0.1 our necessary sample size.

For the qualitative rankings we use a pair-wise similarity metric and Levenshtein distance with substitution cost at unit. Our similarity metric works by first placing a descending order on token's in terms of their log probabilities. Higher in the order means a token has higher probability relative to its peers for that place. We acquire these probabilities directly from a log softmax over the model's logits and from the

Model	JSD-Train μ	JSD-No-train μ	T-Statistic	p-value	0.95 CI
NADE	0.015	0.002	97.594	0.0	(0.004, 0.031)
Transformer	0.156	0.037	325.517	0.0	(0.072, 0.255)
Dec.-Trans.	0.255	0.042	535.584	0.0	(0.113, 0.407)
Switch-Trans.	0.292	0.037	402.528	0.0	(0.151, 0.451)

Table 7: Tests for the Markov property of the learned probability distributions. The average Jensen-Shannon Divergence across samples is presented for trained models and non-trained models. Closer to 0 means more similar. T-tests were conducted between the two models to check whether model is learning, along with 0.95 confidence intervals on the means. $N = 6388$ samples drawn from the training and test distribution (80/20 split) for these tests.

corresponding row in the correct stochastic matrix. After ranking the tokens, we then start with the model's rankings R_m and proceed down the rank. At each token t_j, we take the set of all tokens lower in the ranking $T_m = \{t_i \in R_m : i < j\}$ and intersect that with all tokens lower than t_j in the stochastic matrix ranking R_d, $T_d = \{t_i \in R_d : i < j\}$. We use the cardinality of this set and divide it by the cardinality of the set R_m and this provides our pairwise similarity measure for token t_j:

$$s(t_i) = \begin{cases} \frac{|T_m \cap T_d|}{|T_m|} & \text{if } |T_m| > 0 \\ 0 & \text{otherwise} \end{cases} \tag{6}$$

The similarity S of the two rankings R_m, R_d with k tokens is the sum over these pairwise rankings divided by the k:

$$S(R_m, R_d) = \frac{1}{k} \sum_{j=1}^{k} s(t_j) \tag{7}$$

Finally, the similarity for the whole sequence of length n is simply the sum of the rankings for each member of the sequence divided by n.

Dataset	Trained Model	Untrained Model
Permutation Data	(1.836, 1.968)	(0.533, 0.571)
Random Data	(2.181, 2.338)	(0.540, 0.579)

Table 8: 95% Confidence Intervals on Variance using Chi-Square Test for NADE Models

Dataset	Confidence Interval	Credibility Interval	HDI Interval
Trained Permutation	(-0.098, 0.088)	(-0.098, 0.090)	(-0.098, 0.089)
Trained Random	(-0.135, 0.086)	(-0.136, 0.087)	(-0.138, 0.084)
Untrained Permutation	(-0.099, -0.045)	(-0.099, -0.045)	(-0.100, -0.046)
Untrained Random	(-0.032, 0.022)	(-0.033, 0.022)	(-0.032, 0.023)

Table 9: Comparison of Different Interval Estimates for NADE Models

Bounds	Dataset	T-Stat Lower	P-Value Lower	T-Stat Higher	P-Value Higher
(-0.1, 0.1)	Permutation	2.001	0.023	-2.207	0.014
	Random	1.335	0.091	-2.208	0.014
(-0.25, 0.25)	Permutation	5.157	1.41e-7	-5.363	4.70e-8
	Random	3.992	3.43e-5	-4.864	6.30e-7
(-0.5, 0.5)	Permutation	10.417	6.24e-25	-10.623	8.13e-26
	Random	8.420	4.14e-17	-9.293	2.39e-20
(-1.0, 1.0)	Permutation	20.937	1.66e-86	-21.142	5.60e-88
	Random	17.276	9.62e-62	-18.149	2.26e-67

Table 10: Hypothesis Test Results for Trained NADE Model

Bounds	Dataset	T-Stat Lower	P-Value Lower	T-Stat Higher	P-Value Higher
(-0.1, 0.1)	Permutation	2.001	0.023	-12.502	1.39e-34
	Random	6.794	7.65e-12	-7.511	4.87e-14
(-0.25, 0.25)	Permutation	12.878	1.77e-36	-23.379	1.66e-104
	Random	17.523	2.56e-63	-18.239	5.75e-68
(-0.5, 0.5)	Permutation	31.007	6.13e-166	-41.508	2.32e-256
	Random	35.404	1.85e-203	-36.121	1.21e-209
(-1.0, 1.0)	Permutation	67.263	0	-77.765	0
	Random	71.167	0	-71.883	0

Table 11: Hypothesis Test Results for Untrained NADE Model

Dataset	Trained Model	Untrained Model
Permutation Data	(0.675, 0.723)	(1.370, 1.468)
Random Data	(6.444, 6.907)	(6.124, 6.564)

Table 12: 95% Confidence Intervals for Variance Using Chi-Square Test for Encoder-Decoder Transformer

Dataset	Confidence Interval	Credibility Interval	HDI Interval
Trained Permutation	(-0.073, -0.005)	(-0.073, -0.004)	(-0.073, -0.004)
Trained Random	(-0.340, 0.314)	(-0.339, 0.315)	(-0.327, 0.323)
Untrained Permutation	(-0.150, -0.011)	(-0.150, -0.010)	(-0.152, -0.013)
Untrained Random	(-0.197, 0.424)	(-0.194, 0.427)	(-0.191, 0.429)

Table 13: Comparison of Different Interval Types Across Models for Encoder-Decoder Transformer

Bounds	Dataset	T-Stat Lower	P-Value Lower	T-Stat Higher	P-Value Higher
(-0.1, 0.1)	Permutation	3.502	2.37e-4	-7.952	1.72e-15
	Random	0.521	0.301	-0.678	0.249
(-0.25, 0.25)	Permutation	12.093	1.42e-32	-16.542	3.70e-57
	Random	1.420	0.078	-1.577	0.057
(-0.5, 0.5)	Permutation	26.410	3.86e-128	-30.860	1.05e-164
	Random	2.919	0.002	-3.076	0.001
(-1.0, 1.0)	Permutation	55.045	0	-59.495	0
	Random	5.917	2.00e-9	-6.074	7.76e-10

Table 14: Hypothesis Test Results for Trained Model Encoder-Decoder Transformer

Bounds	Dataset	T-stat Lower	P-value Lower	T-stat Higher	P-value Higher
(-0.1, 0.1)	Permutation	0.555	0.290	-5.087	2.04e-7
	Random	1.345	0.089	0.083	0.533
(-0.25, 0.25)	Permutation	4.786	9.30e-7	-9.318	1.91e-20
	Random	2.291	0.011	-0.863	0.194
(-0.5, 0.5)	Permutation	11.838	2.38e-31	-16.370	4.25e-56
	Random	3.869	5.69e-5	-2.441	0.007
(-1.0, 1.0)	Permutation	25.941	2.11e-124	-30.473	1.85e-161
	Random	7.023	1.60e-12	-5.595	1.29e-8

Table 15: Hypothesis Test Results for Untrained Model Encoder-Decoder Transformer

Dataset	Trained Model	Untrained Model
Permutation Data	(0.9685, 1.0380)	(1.9657, 2.1068)
Random Data	(6.6090, 7.0837)	(6.5223, 6.9907)

Table 16: 95% Confidence Intervals for Variance Using Chi-Square Test for Decoder-only Transformer

Dataset	Confidence Interval	Credibility Interval	HDI Interval
Trained Permutation	(-0.4987, -0.4005)	(-0.4980, -0.4001)	(-0.4987, -0.4008)
Trained Random	(-0.3885, 0.2818)	(-0.3844, 0.2810)	(-0.3821, 0.2824)
Untrained Permutation	(-0.1519, 0.0475)	(-0.1519, 0.0497)	(-0.1501, 0.0512)
Untrained Random	(-0.3930, 0.2685)	(-0.3930, 0.2690)	(-0.3888, 0.2716)

Table 17: Comparison of Different Interval Types Across Models for Decoder-only Transformer

Bounds	Dataset	T-Stat Lower	P-Value Lower	T-Stat Higher	P-Value Higher
(-0.1, 0.1)	Permutation	-13.9481	1.0000	-21.9268	1.13e-93
	Random	0.2725	0.3926	-0.8967	0.1850
(-0.25, 0.25)	Permutation	-7.9641	1.0000	-27.9108	2.92e-140
	Random	1.1494	0.1253	-1.7736	0.0382
(-0.5, 0.5)	Permutation	2.0093	0.0223	-37.8841	6.54e-225
	Random	2.6109	0.0046	-3.2350	0.0006
(-1.0, 1.0)	Permutation	21.9560	6.87e-94	-57.8308	0.0000
	Random	5.5339	1.83e-8	-6.1580	4.65e-10

Table 18: Hypothesis Test Results for Trained Model Decoder-only Transformer

Bounds	Dataset	T-Stat Lower	P-Value Lower	T-Stat Higher	P-Value Higher
(-0.1, 0.1)	Permutation	0.9396	0.1738	-2.9914	0.0014
	Random	0.2237	0.4115	-0.9610	0.1683
(-0.25, 0.25)	Permutation	3.8880	5.26e-5	-5.9397	1.75e-9
	Random	1.1123	0.1331	-1.8496	0.0323
(-0.5, 0.5)	Permutation	8.8018	1.71e-18	-10.8536	7.88e-27
	Random	2.5932	0.0048	-3.3305	0.0004
(-1.0, 1.0)	Permutation	18.6295	1.50e-70	-20.6813	1.10e-84
	Random	5.5551	1.62e-8	-6.2923	2.01e-10

Table 19: Hypothesis Test Results for Untrained Model Decoder-only Transformer

Dataset	Trained Model	Untrained Model
Permutation Data	(0.7601, 0.8147)	(3.6449, 3.9067)
Random Data	(6.4088, 6.8691)	(10.1253, 10.8525)

Table 20: 95% Confidence Intervals for Variance Using Chi-Square Test for Switch Transformer

Dataset	Confidence Interval	Credibility Interval	HDI Interval
Trained Permutation	(0.0331, 0.1102)	(0.0327, 0.1099)	(0.0324, 0.1095)
Trained Random	(-0.4135, 0.2365)	(-0.4121, 0.2303)	(-0.4018, 0.2374)
Untrained Permutation	(-0.5226, -0.1529)	(-0.5219, -0.1523)	(-0.5246, -0.1554)
Untrained Random	(-0.2136, 0.8133)	(-0.2065, 0.7967)	(-0.2134, 0.7866)

Table 21: Comparison of Different Interval Types Across Models for Switch Transformer

Bounds	Dataset	T-Stat Lower	P-Value Lower	T-Stat Higher	P-Value Higher
(-0.1, 0.1)	Permutation	8.723	3.34e-18	-1.443	7.46e-2
	Random	0.069	4.72e-1	-1.136	1.28e-1
(-0.25, 0.25)	Permutation	16.347	5.80e-56	-9.067	1.74e-19
	Random	0.974	1.65e-1	-2.041	2.07e-2
(-0.5, 0.5)	Permutation	29.055	1.18e-149	-21.774	1.47e-92
	Random	2.481	6.61e-3	-3.548	2.00e-4
(-1.0, 1.0)	Permutation	54.469	0	-47.189	2.16e-305
	Random	5.495	2.27e-8	-6.562	3.57e-11

Table 22: Hypothesis Test Results for Trained Model Switch Transformer

Bounds	Dataset	T-Stat Lower	P-Value Lower	T-Stat Higher	P-Value Higher
(-0.1, 0.1)	Permutation	-2.520	9.94e-1	-4.640	1.89e-6
	Random	1.526	6.36e-2	0.763	7.77e-1
(-0.25, 0.25)	Permutation	-0.930	8.24e-1	-6.230	2.98e-10
	Random	2.098	1.80e-2	0.190	5.75e-1
(-0.5, 0.5)	Permutation	1.720	4.28e-2	-8.880	8.80e-19
	Random	3.052	1.15e-3	-0.764	2.23e-1
(-1.0, 1.0)	Permutation	7.020	1.63e-12	-14.180	2.23e-43
	Random	4.960	3.90e-7	-2.672	3.81e-3

Table 23: Hypothesis Test Results for Untrained Model Switch Transformer

Model	Train μ	Train σ	0.95 CI Train	No-train μ	No-train σ	0.95 CI No-train
Transformer	3.07	1.42	(3.00, 3.14)	-5.67	1.63	(-5.75, -5.59)
Decoder-Trans.	3.25	1.29	(3.19, 3.32)	-6.11	1.93	(-6.21, -6.02)
Switch-Trans.	4.05	1.50	(3.98, 4.13)	-5.51	1.85	(-5.60, -5.42)

Table 24: Tests for comparing the difference in the log probability assigned by a model and the true log probability of the sequence (LD). We observe that all three model architectures show significant > 1 average differences with large standard deviations. We also observe that this differs markedly from the non-trained models, which are significantly underconfident relative to the true probabilities.